Title

Excitation of dayside chorus waves due to magnetic field line compression in response to interplanetary shocks

Journal

Journal of Geophysical Research Space Physics, 120(10)

ISSN

2169-9380

Authors

Zhou, Chen
Li, Wen
Thorne, Richard M
et al.

Publication Date

2015-10-01

DOI

10.1002/2015ja021530

Peer reviewed

AGU PUBLICATIONS

JGR

Journal of Geophysical Research: Space Physics

RESEARCH ARTICLE
10.1002/2015JA021530

Key Points:
- Excitation of dayside chorus waves is observed
- These waves are in response to IP shocks
- IP shocks change the magnetic field line configuration

Correspondence to:
C. Zhou,
chenzhou@whu.edu.cn

Citation:
Zhou, C., et al. (2015), Excitation of dayside chorus waves due to magnetic field line compression in response to interplanetary shocks, *J. Geophys. Res. Space Physics*, *120*, doi:10.1002/2015JA021530.

Received 2 JUN 2015
Accepted 3 SEP 2015
Accepted article online 7 SEP 2015

Excitation of dayside chorus waves due to magnetic field line compression in response to interplanetary shocks

Chen Zhou[1,2,3], Wen Li[2], Richard M. Thorne[2], Jacob Bortnik[2], Qianli Ma[2], Xin An[2], Xiao-jia Zhang[2,4], Vassilis Angelopoulos[4,5], Binbin Ni[1,3], Xudong Gu[1], Song Fu[1], and Zhengyu Zhao[1]

[1]Department of Space Physics, School of Electronic Information, Wuhan University, Wuhan, China, [2]Department of Atmospheric and Oceanic Sciences, University of California, Los Angeles, California, USA, [3]State Key Laboratory of Space Weather, Chinese Academy of Sciences, Beijing, China, [4]Department of Earth, Planetary, and Space Sciences, University of California, Los Angeles, California, USA, [5]Institute of Geophysics and Planetary Physics, Department of Earth and Space Sciences, University of California, Los Angeles, California, USA

Abstract The excitation of magnetospheric whistler-mode chorus in response to interplanetary (IP) shocks is investigated using wave data from the Time History of Events and Macroscale Interactions during Substorms (THEMIS) spacecraft. As an example, we show a typical chorus wave excitation following an IP shock event that was observed by THEMIS in the postnoon sector near the magnetopause on 3 August 2010. We then analyze characteristic changes during this event and perform a survey of similar events during the period 2008–2014 using the THEMIS and OMNI data set. Our statistical analysis demonstrates that the chorus wave excitation/intensification in response to IP shocks occurs only at high L shells ($L > 8$) on the dayside. We analyzed the variations of magnetic curvature following the arrival of the IP shock and found that IP shocks lead to more homogeneous background magnetic field configurations in the near-equatorial dayside magnetosphere; and therefore, the threshold of nonlinear chorus wave growth is likely to be reduced, favoring chorus wave generation. Our results provide the observational evidence to support the concept that the geomagnetic field line configuration plays a key role in the excitation of dayside chorus.

1. Introduction

Magnetospheric whistler-mode chorus waves are right-handed elliptically polarized electromagnetic emissions, which play an important role in radiation belt electron dynamics [*Burtis and Helliwell*, 1976; *Tsurutani and Smith,* 1974, 1977; *Meredith et al.,* 2001; *Thorne,* 2010; *Li et al.,* 2012]. Frequency spectra of magnetospheric chorus waves have been characteristically divided into two bands 0.1–0.5 f_{ce} and 0.5–0.8 f_{ce} with a gap at 0.5 f_{ce}, where f_{ce} is the equatorial electron gyrofrequency. Chorus waves are believed to cause enhancements of relativistic electron fluxes via wave-particle interactions [*Horne and Thorne*, 2003; *Horne et al.,* 2005; *Bortnik et al.,* 2007; *Ni et al.,* 2008, 2011a, 2011b, 2014; *Thorne et al.,* 2013; *Li et al.,* 2007, 2008, 2014; *Tu et al.,* 2014]. Chorus waves also modify the electron pitch angle distribution and scatter plasma sheet electrons into the loss cone, thereby causing the precipitation loss to form the diffuse and pulsating auroras [*Horne and Thorne,* 1998; *Shprits et al.,* 2006; *Tsurutani et al.,* 2009; *Ni et al.,* 2011b, 2014; *Nishimura et al.,* 2010, 2013; *Thorne et al.,* 2010; *Summers et al.,* 1998, 2002]. Besides the dual role it plays in both acceleration and loss of radiation belt electrons, magnetospheric chorus acts as an important source of plasmaspheric hiss [*Bortnik et al.,* 2008, 2009a, 2009b].

Generation of chorus waves is generally attributed to the wave-particle interaction of noise-level seed waves with anisotropic electrons having energies between a few and tens of keV [e.g., *Kennel and Petschek,* 1966; *Kennel and Thorne,* 1967; *Tsurutani and Smith,* 1974; *Nunn et al.,* 1997; *Chum et al.,* 2007; *Katoh and Omura,* 2007a, 2007b; *Omura et al.,* 2008; *Omura and Nunn*, 2011; *Tao,* 2014]. While the mechanism(s) responsible for the chorus excitation has been a subject of intense research [e.g., *Omura et al.,* 2008, 2009; *Bespalov et al.,* 2010; *Schriver et al.,* 2010; *Lampe et al.,* 2010; *Demekhov,* 2011; *Katoh and Omura,* 2013; *Tao,* 2014; *Mourenas et al.,* 2015; *Nunn and Omura,* 2015], further investigation is required to understand chorus generation with various wave normal angles and emission types (i.e., rising/falling tone and hiss-like emission) [*Santolík et al.,* 2009; *Li et al.,* 2011; *Gao et al.,* 2014].

Previous statistical studies of the global distribution of chorus waves show that chorus wave properties are strongly dependent on the spatial location and the level of geomagnetic activity [e.g., *Tsurutani and Smith,* 1977; *Parrot and Gaye,* 1994; *Meredith et al.,* 2003, 2014; *Santolík et al.*, 2003, 2005]. According to a comprehensive global survey of magnetospheric chorus wave distribution [*Li et al.,* 2009a, 2009b; *Meredith et al.,* 2012], chorus waves at low latitudes or near-equatorial region present an obvious day-night asymmetry. Dayside chorus shows persistently high occurrence rates even during geomagnetically quiet times. Distinct from the nightside chorus excitation related to substorm activity, the generation mechanism of dayside chorus remains an open question.

Spasojevic and Inan [2010] performed a statistical analysis by using ELF/VLF wave data from two Antarctic ground stations. By investigating the occurrence rate, amplitudes, and drivers of magnetospheric chorus waves, they reported that chorus waves in the noon sector are less dependent on geomagnetic activity and are occasionally observed even during quiet conditions, which they attributed to the anisotropic electron distributions due to drift shell splitting and more homogeneous background magnetic field due to the solar wind compression of the dayside magnetosphere. *Keika et al.* [2012] also performed a case study of chorus waves on the dayside observed by Time History of Events and Macroscale Interactions during Substorms (THEMIS) satellites and ground-based ELF/VLF receivers. They found that the nearly uniform field ($dB/ds \sim 0$) is favorable for the existence of long-lasting, localized, quiet time dayside chorus waves. Both studies imply the importance of the background magnetic field line configuration to the chorus excitation from an observational perspective.

Katoh and Omura [2013] studied the effect of the background magnetic field inhomogeneity on the generation process of whistler-mode chorus emissions using self-consistent electron hybrid code simulations. They found that the small spatial inhomogeneity of the ambient magnetic field results in a small threshold amplitude for the nonlinear growth rate which allows the triggering process to occur more easily. *Tao et al.* [2014] carried out a similar investigation on the day-night asymmetry of chorus occurrence rate and also found that the nearly uniform magnetic field on the dayside significantly lowers the threshold condition for chorus excitation, while the stretched nightside magnetic field requires a higher value of temperature anisotropy or hot electron number density to generate chorus.

Fu et al. [2012] studied a chorus intensification event in the dayside magnetosphere on 3 September 2009. They claimed that due to the interplanetary (IP) shock compression, the temperature anisotropy of electrons was enhanced, which could make the chorus intensification very effective. In addition to this effect, we expect that the IP shock compression can potentially modify the magnetic field line configuration on the dayside, which needs further investigation to understand the underlying influence of the geomagnetic field line homogeneity on the chorus wave excitation.

The purpose of this study is to investigate the chorus wave excitation in response to interplanetary (IP) shocks in a statistical sense. By using wave observations from the Time History of Events and Macroscale Interactions during Substorms (THEMIS) spacecraft, we aim to identify the preferential locations of chorus wave excitation and to understand the physical factors accounting for the chorus wave excitation in association with an IP shock.

The outline of this paper is as follows. In section 2, we give a brief description of the data and methodology used for investigating the responses of chorus waves to IP shocks. A detailed case study is presented in section 3. A typical interplanetary shock is identified, and the simultaneous THEMIS spacecraft observations are described. In section 4, we present the statistical results for the period of 2008–2014 and our superposed epoch analysis results. In section 5, we further discuss the chorus wave excitation/intensification in response to IP shocks followed by the summary in section 6.

2. Data and Methodology

The THEMIS mission consists of five satellites in near-equatorial orbits with apogees above 10 R_E and perigees below 2 R_E [*Angelopoulos,* 2008]. The locations of the THEMIS satellites are ideally situated to investigate magnetospheric chorus emissions since these are typically generated near the equator and can include key parameters such as background magnetic field, total electron density, and electron pitch angle distributions. In this study, data from only three satellites, THEMIS A (ThA), THEMIS D (ThD), and THEMIS E (ThE) are included since they are mostly located in the inner magnetosphere. Data from the Electric Field Instrument (EFI),

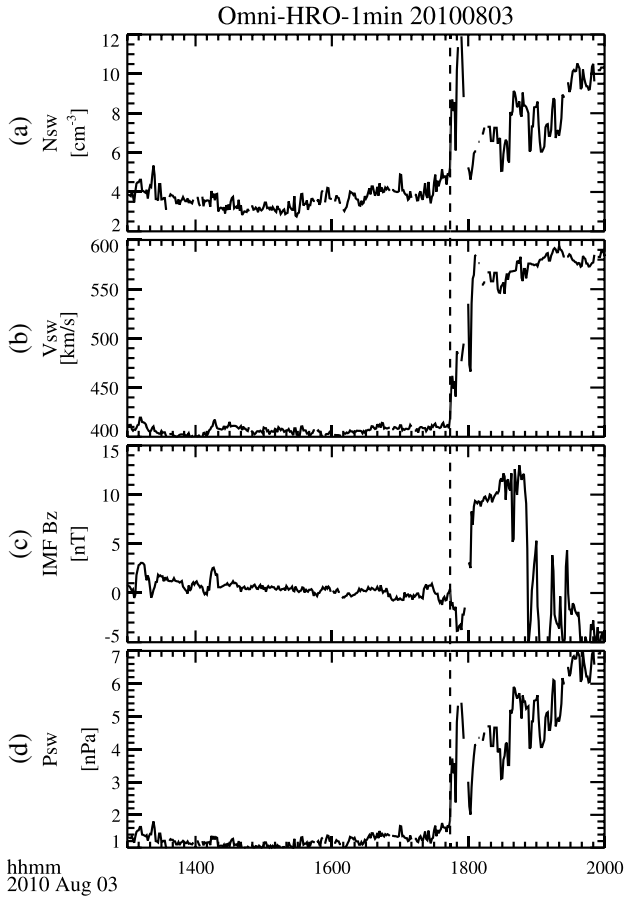

Figure 1. Solar wind and IMF parameters obtained from OMNI-HRO 1 min data. (a) The solar wind density, (b) solar wind velocity, (c) IMF B_z, and (d) solar wind dynamic pressure are illustrated, respectively. The dashed line indicates the approximate arrival time of an interplanetary shock, which is 17:40 UT on 3 August 2010.

Search Coil Magnetometer (SCM), Fluxgate Magnetometer (FGM), and electrostatic analyzer (ESA) are used. The EFI measures the waveforms and three-axis spectra of the ambient electric fields from DC up to 8 kHz [*Bonnell et al.,* 2008]. The SCM measures low-frequency magnetic field fluctuations and waves in three orthogonal directions over a frequency range from 0.1 Hz to 4 kHz [*Le Contel et al.,* 2008; *Roux et al.,* 2008]. The EFI and SCM output waveforms are digitized and processed by the Digital Fields Board [*Cully et al.,* 2008]. The FGM measures background magnetic fields and their low-frequency fluctuations (up to 64 Hz) [*Auster et al.,* 2008]. The ESA collects the electron pitch angle distribution data for energies ranging from a few eV up to 30 keV. Furthermore, total electron density can be inferred from the spacecraft potential measured by EFI and electron thermal velocity measured by ESA [*Li et al.,* 2010b]. Equipped with high-quality and high-performance electric field (EFI), magnetic field (SCM), and particle (ESA) instruments, the THEMIS satellites provide an excellent opportunity to study chorus waves and their response to interplanetary shocks.

High-resolution OMNI data are obtained from the OMNI website (ftp://spdf.gsfc.nasa.gov/pub/data/omni/high_res_omni/). The proton density, solar wind flow speed, interplanetary magnetic field (IMF) B_z in GSM coordinates, and solar wind pressure are selected to identify the arrival time of a shock. Since the resolution of OMNI-HRO data is 1 min, the IP shock events identified in this study have an inherent 1 min accuracy.

3. Event Study: THEMIS Observation During an IP Shock

Figure 1 shows the solar wind and IMF conditions from 13:00 to 20:00 UT on 3 August 2010. Figures 1a–1d show the solar wind density, solar wind velocity, IMF B_z in GSM coordinates, and solar wind dynamic pressure, respectively. Between 17:40 and 17:41 UT (around the vertical dashed line), the solar wind density increased from 5 to 12 cm^{-3}, the solar wind velocity increased from 410 to 580 km/s, IMF B_z decreased from 0 to −5 nT, and the solar wind dynamic pressure increased from 1.5 to 5 nPa, all of which indicate typical features of an interplanetary shock [e.g., *Yue et al.,* 2010; *Yue and Zong*, 2011; *Zong et al.,* 2009].

Figure 2 shows the chorus wave intensification observed between 17:38 and 17:42 UT on 3 August 2010 by THEMIS A at magnetic local time (MLT) ~15.7 and L shell ~9.5. Figure 2a shows the total electron density inferred from the THEMIS spacecraft potential. Figure 2b shows the total magnetic field B_{tot} (black) and the z component B_z (red) in the solar magnetic coordinate system. Note that B_z was almost the same as B_{tot}, indicating that the total variation in the ambient magnetic field mainly occurred in the z direction. Figure 2c illustrates the evolution of omnidirectional electron energy fluxes at energies from 10 eV to 30 keV. Figures 2d

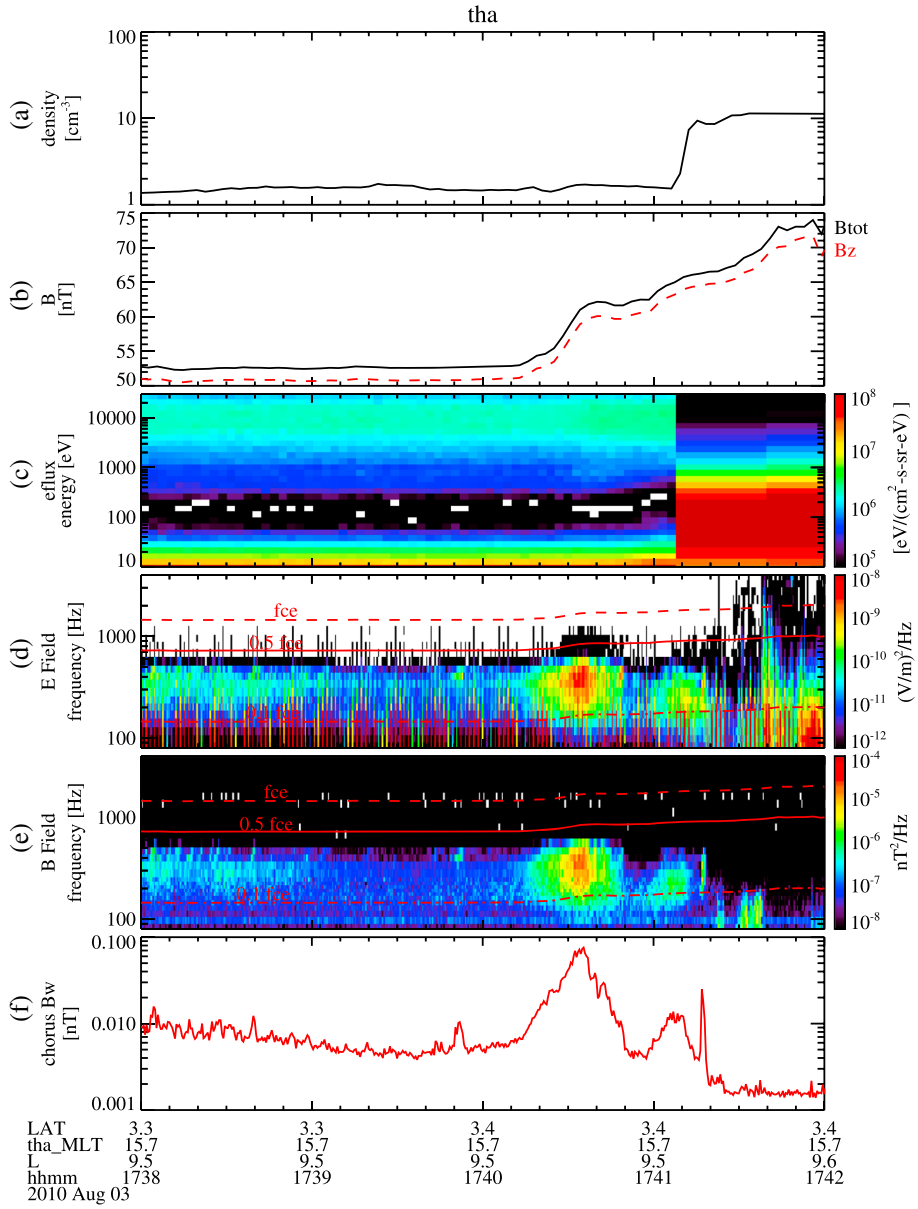

Figure 2. Chorus wave excitation observed by THEMIS A between 17:36:00 and 17:42:00 UT on 3 August 2010, showing (a) total electron density, (b) background magnetic field intensity in total (black) and in the *z* direction (red), (c) omnidirectional electron energy flux, (d) frequency-time spectrogram in electric field, (e) magnetic field, and (f) chorus wave amplitude. The three lines in Figures 2d and 2e represent 1 f_{ce} (dashed), 0.5 f_{ce} (solid), and 0.1 f_{ce} (dashed dotted).

and 2e show the time-frequency spectrograms of the wave electric and magnetic components during the interval using the SCM particle-burst mode data. Chorus wave amplitudes (B_w) calculated as the integral of wave magnetic spectral density between 0.1 and 0.8 f_{ce} are plotted in Figure 2f. The local electron cyclotron frequency is first obtained from the ambient magnetic field measured by the FGM instrument on board THEMIS and then converted to the equatorial electron cyclotron frequency f_{ce} based on a dipole magnetic field model.

THEMIS A was inside the magnetopause when the shock occurred and provided fairly good measurements of plasma waves and particle distributions near the dayside. As shown in Figure 2, shortly after the shock impinging at the dayside magnetopause around 17:40:10 UT, the background magnetic field began increasing (Figure 2b) due to the IP shock compressional effect [e.g., *Yue et al.*, 2009, 2011]. Figures 2d and 2e also

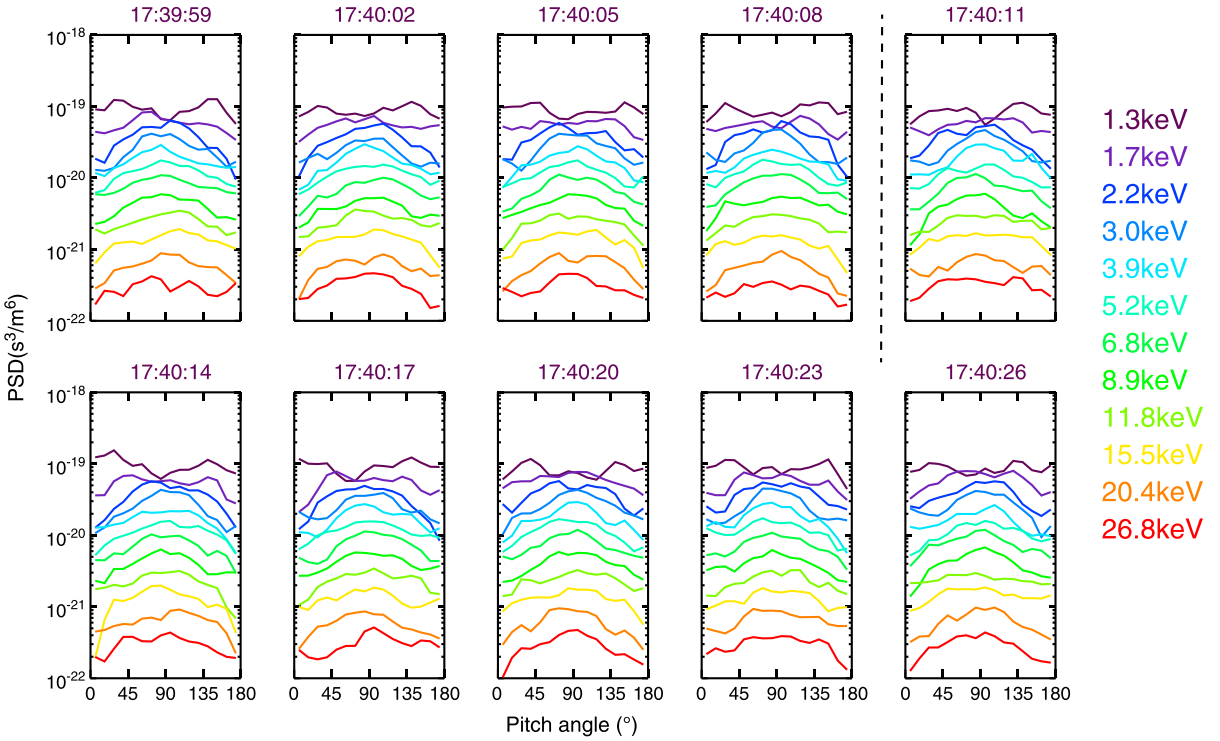

Figure 3. The time evolution of electron phase space density as a function of pitch angle for 12 different energy levels measured by THEMIS A from 17:39:59 UT to 17:40:26 UT with an accumulation time of 3 s.

show the enhancement of the wave electric and magnetic components in the spectrogram. The excited waves occurred at frequencies between 0.1 and 0.5 f_{ce}, indicating a typical lower band whistler-mode chorus wave signature. Figure 2f shows that the excited chorus wave amplitudes increased substantially from ~7 to ~80 pT. However, significant changes in electron density (Figure 2a) and electron energy flux (Figure 2c) were not observed before ~17:41:10 UT.

In order to examine whether this chorus wave intensification was induced by changes in the anisotropy of electron pitch angle distribution, we show in Figure 3 the time evolution of the electron phase space density as a function of pitch angle for 12 different energy channels from 1.3 to 26.8 keV having an accumulation time of 3 s. We also calculate the minimum resonant energy for the cyclotron resonance [*Li et al.*, 2010a] and find that it is less than 20 keV during the period concerned, indicating that electron measurements obtained from ESA could give essential information of the energetic electrons that provide a source of free energy for chorus excitation. The vertical black dashed line in Figure 3 indicates the approximate starting time of background magnetic field increase. However, no significant changes in electron pitch angle distribution are observed before and after the black dashed line, which implies that the electron anisotropy remains essentially unchanged after the IP shock impact.

In summary, in this event, which occurred at a large L shell (~9.5) in the afternoon sector, an obvious chorus intensification was observed in response to the IP shock, along with an increase in the background magnetic field. However, the electron pitch angle distribution did not exhibit a significant change, so the chorus was not likely excited due to an increase in the available free energy but likely due to a decrease in the threshold required to excite chorus.

4. Statistical Analysis of Chorus Wave Excitation During IP Shock Events

In order to comprehensively investigate the chorus wave excitation in response to IP shocks, we analyzed 20 IP shock events that occurred between 1 January 2008 and 31 December 2014, which have simultaneous observations of chorus made by THEMIS A, THEMIS D, and THEMIS E. During this 7 year period, the THEMIS spacecraft provide excellent coverage in MLT and L shell.

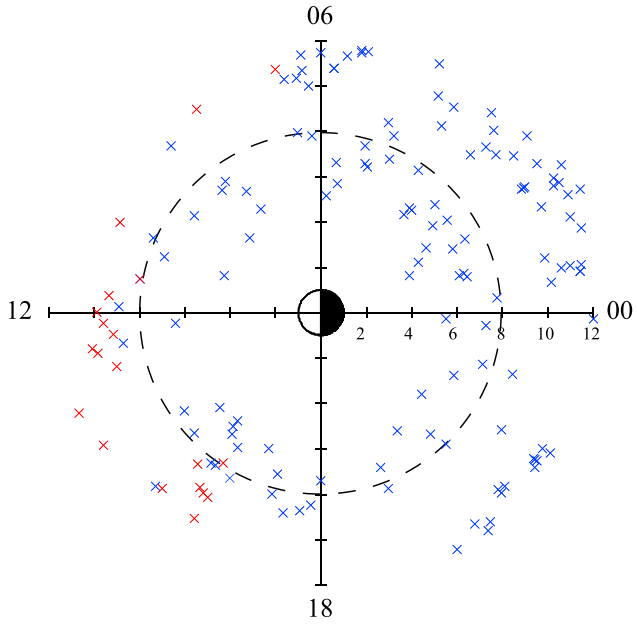

Figure 4. Locations of THEMIS satellites mapped into the equatorial magnetosphere when the IP shock arrived. Red crosses indicate the locations of satellites with chorus wave intensification/excitation. Blue crosses indicate the locations of satellites without chorus wave intensification/excitation.

Figure 4 shows the combined locations of all three THEMIS satellites when an IP shock arrived during the period between 1 January 2008 and 31 December 2014. The red crosses are the locations of the spacecraft where clear chorus wave excitation or intensification events were observed, while the blue crosses are the locations of the spacecraft which did not observe chorus wave excitation or intensification. Events with chorus wave excitation/intensification were identified if chorus wave amplitudes increased at least by a factor of 2 in 1 min after the shock arrival. Twenty IP shock events associated with chorus wave excitation/intensification are identified during this period. The universal time, MLT, and L shell of these 20 events are listed in Table 1. Figure 4 demonstrates that the chorus wave excitation/intensification in response to IP shocks preferentially occurs at high L shells (larger than 8) and on the dayside (MLT from 6 to 18), which may be close to the dayside magnetopause. By using the model introduced by *Shue et al.* [1997, 1998], we calculate the distances to the magnetopause of all probes with chorus wave excitation/intensification as the IP shock arrival. The root-mean-square value is ~1.5 R_E, which indicates that all the probes with chorus wave excitation/intensification are located quite near the magnetopause. It is interesting to note that, if the chorus wave excitation/intensification induced by the same IP shock is observed by two or three probes, the wave characteristics are very similar. However, we did find two events where the spacecraft were close to each other and one satellite captured the chorus intensification but the other did not. This provides some information about the spatial distribution of the excited chorus waves.

Table 1. A Summary of Chorus Intensification/Excitation Events in Response to IP Shocks During 2008–2014

No	Time	Probe	L shell	MLT
1	2014-06-07/16:52:00	a	10.6	8.1
2	2014-06-07/16:52:00	d	11	6.7
3	2014-03-25/20:03:00	e	9.8	10.4
4	2014-02-20/03:19:00	d	9.5	11.7
5	2014-02-19/03:47:00	d	8.2	11.3
6	2014-02-13/09:43:00	a	10.3	12.6
7	2014-02-13/09:43:00	e	11.4	14.1
8	2014-02-07/08:11:00	d	11.7	13.5
9	2011-11-12/05:58:00	a	8.7	15.4
10	2011-11-12/05:58:00	d	8.1	15.8
11	2010-08-03/17:40:00	a	9.5	15.7
12	2010-08-03/17:40:00	d	9.7	15.9
13	2010-08-03/17:40:00	e	9.6	15.8
14	2009-10-11/00:28:00	d	9.4	13.0
15	2009-10-11/00:28:00	e	10.1	12.7
16	2009-09-03/15:51:00	a	10	12
17	2009-09-03/15:51:00	d	9.3	12.4
18	2009-09-03/15:51:00	e	9.7	12.2
19	2008-06-24/20:09:00	a	10.8	15.9
20	2008-06-24/20:09:00	e	10.6	15.2

To investigate the chorus wave intensification/excitation in response to IP shocks comprehensively, we conduct a superposed epoch analysis of the selected 20 IP shock events associated with chorus wave excitation/intensification. In the superposed epoch analysis, we define the zero epoch time as the time when the background total magnetic field begins to increase. The statistical results are shown in Figure 5 for the normalized hot (1–30 keV) plasma density (Figure 5a), the normalized total electron density (Figure 5b), the normalized background total magnetic field (Figure 5c), and the chorus wave power (Figure 5d), respectively.

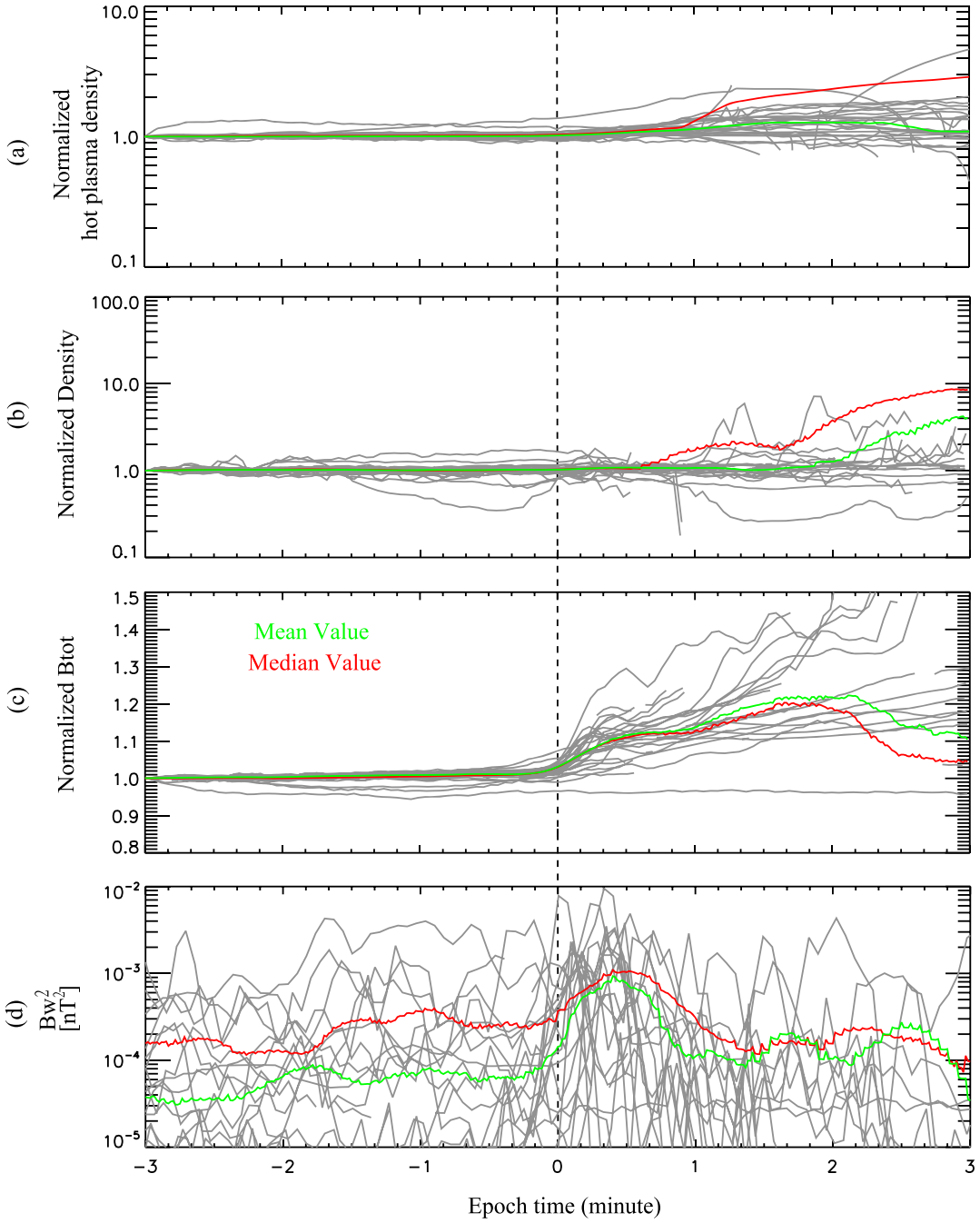

Figure 5. Superposed epoch analysis results of 20 chorus intensification/excitation events showing (a) omnidirectional electron energy flux, (b) total electron density, (c) normalized background magnetic field, and (d) chorus wave energy. Dashed line indicates the approximate arrival time of an interplanetary shock. The green and red lines are the mean and median value of the 20 events.

The green and red lines are the mean and median values of the 20 events. The hot plasma density, total electron density, and background total magnetic field are normalized to the values at 3 min before the zero epoch time.

From the statistical analysis shown in Figure 5, we find that in association with the IP shocks, chorus wave excitation/intensification is clearly observed at high L shells on the dayside along with an enhancement of the background magnetic field intensity. However, during the period of chorus wave excitation, the total electron density and hot electron flux remained almost unchanged.

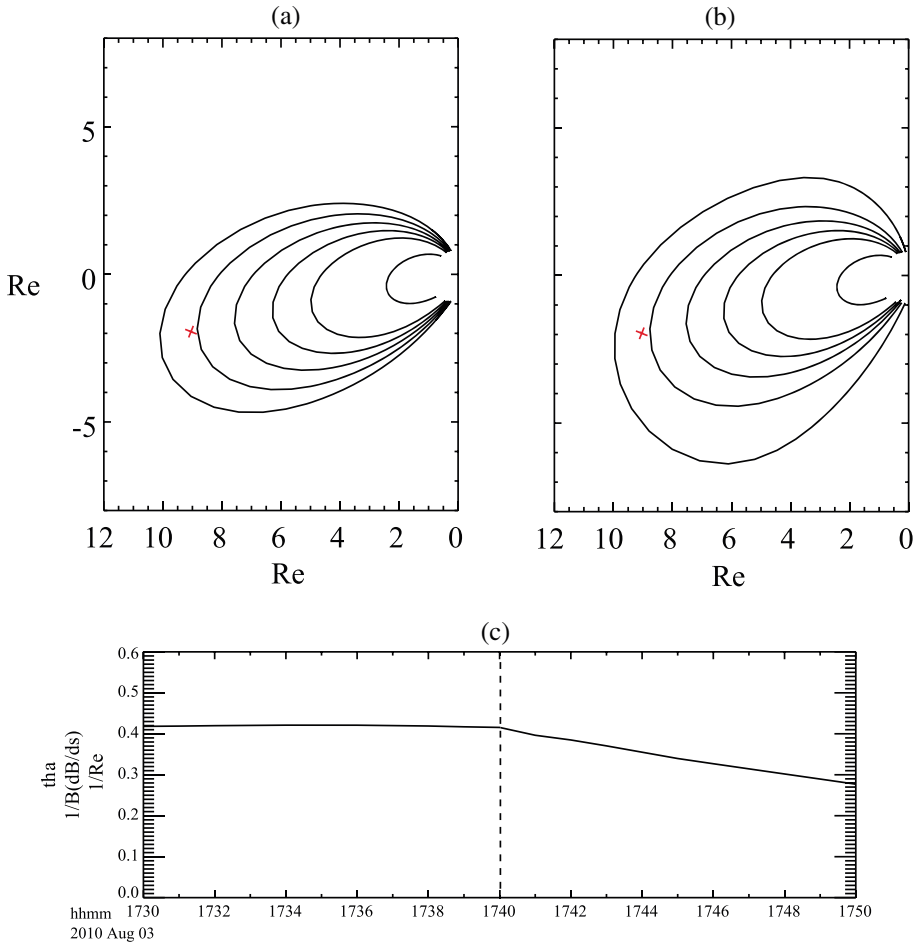

Figure 6. Magnetic field line configuration 1 min (a) before and (b) after the IP shock arrival in the meridian plane, where the red cross is the location of THEMIS A. (c) The time evolution of magnetic field curvature on the equatorial plane for the magnetic field line where THEMIS A is located. Vertical dashed line is the shock arrival time.

5. Discussion

In the above analysis, we focused on the impact of IP shocks on the chorus wave excitation/intensification. The IP shocks are identified from the solar wind and IMF parameters. Using simultaneous measurements from the THEMIS satellites, we examined the chorus wave excitation/intensification in response to IP shocks. We investigated the evolution of total electron density, geomagnetic field, electron flux, wave electric and magnetic field power spectra, wave amplitude, and energetic electron phase space density and found that after the IP shock arrival, clear chorus wave intensification is observed along with an increase in ambient magnetic field intensity while the electron pitch angle distribution shows no significant changes.

Our statistical results indicate that the chorus wave excitation/intensification associated with IP shock impact is typically observed by THEMIS spacecraft at high L shells (>8) on the dayside close to the magnetopause. This is probably because the compressional effect on the magnetic field caused by IP shocks is most significant in that region. By using the Tsyganenko (TS04D) model [*Tsyganenko and Sitnov,* 2005] and OMNI-HRO 1 min data, we plot the magnetic field configuration of the magnetosphere before and after the IP shock arrival for the event shown in Figure 2. To justify the accuracy of this adopted geomagnetic field model, we compared the model results with the ambient magnetic field properties measured by THEMIS A, which shows good agreement with each other. Figure 6a (6b) shows the magnetic field line configuration 1 min before (after) the IP shock arrival in the meridian plane at 15.9 MLT. The red crosses in Figures 6a and 6b indicate the locations of THEMIS A before and after the shock. We find that compared to the magnetic field line configuration before the IP shock, the magnetic field line after the shock appears to be more homogeneous,

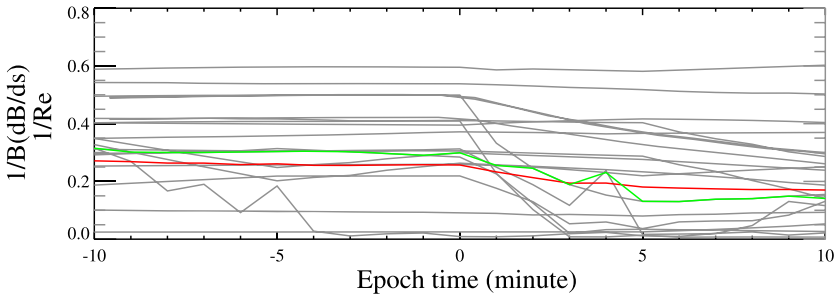

Figure 7. Superposed epoch analysis results of magnetic field curvature (d*B*/d*s*) for the chorus intensification/excitation events.

especially near the magnetospheric equatorial region. In Figure 6c, we calculate the time evolution of magnetic field curvature (1/*B*)(d*B*/d*s*) on the equatorial plane for the magnetic field line where THEMIS A is located. The background magnetic field line curvature is calculated by fitting two quadric surfaces based on TS04D [*Tsyganenko and Sitnov,* 2005]. The dashed line in Figure 6c marks the time when the IP shock arrives. It should be noted that due to the 1 min time resolution of OMNI data, this timing has an uncertainty of up to 1 min. Figure 6c indicates that the curvature of magnetic field decreases after the shock arrival. This decrease is caused by the compressional effect of the IP shock. We have also carried out a superposed epoch analysis of the background magnetic field curvature change during the 20 IP shock events associated with chorus wave excitation/intensification, and the results are shown in Figure 7. The value of d*B*/d*s* decreases after the IP shock arrival for most events, indicating that the magnetic field configuration plays an important role in the chorus wave excitation/intensification.

According to *Omura et al.* [2008], a smaller value of d*B*/d*s* favors the phase trapping of electrons in the potential well of the wave, which is considered a necessary condition for nonlinear wave growth. Our observational results confirm that a more homogeneous field configuration (smaller (1/*B*)(d*B*/d*s*)) is particularly favorable for chorus wave generation, which is consistent with the theoretical studies by *Katoh and Omura* [2013] and *Tao et al.* [2014].

We also point out from Figure 2 that the temporal duration of chorus wave excitation observed by the THEMIS spacecraft only lasts for about 30 s. However, the compressional effects on the magnetic field caused by IP shocks were sustained for at least a few minutes. We suggest that this inconsistency might be because energetic electron distributions are in a marginally stable state on the dayside; and thus, the free energy stored in anisotropic electrons is limited and might be capable of providing chorus wave excitation for a short period (i.e., ~30 s). This marginal instability could potentially account for both the short duration of the chorus bursts and the very small changes in electron pitch angle distributions, which are probably not noticeable in the 3 s averaged THEMIS electron measurements. Therefore, we cannot completely exclude the possibility that chorus intensification in association with IP shocks might be caused by this small change in electron distributions, as suggested by *Fu et al.* [2012], but this change in electron distributions from the present study is indeed smaller than what is reported by *Fu et al.* [2012]. However, a more detailed investigation is beyond the scope of the present study, and a future investigation is required to better understand this inconsistency.

6. Conclusions

In the present study, we have investigated the chorus wave excitation/intensification at high L shells in the dayside magnetosphere in response to IP shocks, using chorus wave data from the THEMIS spacecraft, collected in the near-equatorial magnetosphere. The principal conclusions are summarized as follows:

1. Excitation/intensification of dayside chorus waves is observed without any clear change in anisotropic electron distributions after the IP shock arrival.
2. Based on a statistical survey of THEMIS data from 2008 to 2014, 20 events of chorus wave excitation are identified in close association with IP shocks, and these events characteristically occur at high L shells (>8) in the dayside magnetosphere.

3. Analysis of the geomagnetic field line configurations suggests that a more homogeneous ambient magnetic field configuration could play a key role in the generation/amplification of dayside chorus during a period lasting ~30 s following the IP shock arrival. However, the short duration of the chorus wave relative to the longer period of the reduced curvature of the field line (typically lasting for a few minutes) is beyond the scope of the present study and requires further quantitative investigation.

Acknowledgments
This work was supported by the NSFC grants 41204120 and 41474141, the Fundamental Research Funds for the Central Universities grant 2042014kf0251, and the Project Supported by the Specialized Research Fund for State Key Laboratories. The analysis at UCLA was supported by the NASA grants NNX11AD75G, NNX11AR64G, NNX13AI61G, NNX14AI18G, and NNX15AF61G, and the NSF grants AGS 1405054 and PLR 1341359. We acknowledge the THEMIS data used in this study obtained from http://themis.ssl.berkeley.edu/data/themis/ and the OMNI data obtained from the OMNI website (ftp://spdf.gsfc.nasa.gov/pub/data/omni/high_res_omni/). C.Z. appreciates the support by the China Scholarship Council.

Michael Balikhin thanks the reviewers for their assistance in evaluating this paper.

References

Angelopoulos, V. (2008), The THEMIS mission, *Space Sci. Rev.*, *141*, 5–34, doi:10.1007/s11214-008-9336-1.
Auster, H. U., et al. (2008), The THEMIS fluxgate magnetometer, *Space Sci. Rev.*, *141*, 235–264, doi:10.1007/s11214-008-9365-9.
Bespalov, P. A., M. Parrot, and J. Manninen (2010), Short-period VLF emissions as solitary envelope waves in a magnetospheric plasmamaser, *J. Atmos. Sol. Terr. Phys.*, *72*(17), 1275–1281, doi:10.1016/j.jastp.2010.09.001.
Bonnell, J. W., F. S. Mozer, G. T. Delory, A. J. Hull, R. E. Ergun, C. M. Cully, V. Angelopoulos, and P. R. Harvey (2008), The electric field instrument (EFI) for THEMIS, *Space Sci. Rev.*, *141*(1–4), 303–341, doi:10.1007/s11214-008-9469-2.
Bortnik, J., R. M. Thorne, and N. P. Meredith (2007), Modeling the propagation characteristics of chorus using CRRES suprathermal electron fluxes, *J. Geophys. Res.*, *112*, A08204, doi:10.1029/2006JA012237.
Bortnik, J., R. M. Thorne, and N. P. Meredith (2008), The unexpected origin of plasmaspheric hiss from discrete chorus emissions, *Nature*, *452*(7183), 62–66.
Bortnik, J., W. Li, R. M. Thorne, V. Angelopoulos, C. Cully, J. Bonnell, O. Le Contel, and A. Roux (2009a), An observation linking the origin of plasmaspheric hiss to discrete chorus emissions, *Science*, *324*(5928), 775, doi:10.1126/science.1171273.
Bortnik, J., R. M. Thorne, and N. P. Meredith (2009b), Plasmaspheric hiss overview and relation to chorus, *J. Atmos. Sol. Terr. Phys.*, *71*(16), 1636–1646.
Burtis, W. J., and R. A. Helliwell (1976), Magnetospheric chorus: Occurrence patterns and normalized frequency, *Planet. Space Sci.*, *24*, 1007–1010, doi:10.1016/0032-0633(76)90119-7.
Chum, J., O. Santolík, A. W. Breneman, C. A. Kletzing, D. A. Gurnett, and J. S. Pickett (2007), Chorus source properties that produce time shifts and frequency range differences observed on different Cluster spacecraft, *J. Geophys. Res.*, *112*, A06206, doi:10.1029/2006JA012061.
Cully, C. M., R. E. Ergun, K. Stevens, A. Nammari, and J. Westfall (2008), The THEMIS digital fields board, *Space Sci. Rev.*, *141*(1–4), 343–355, doi:10.1007/s11214-008-9417-1.
Demekhov, A. G. (2011), Generation of VLF emissions with the increasing and decreasing frequency in the magnetospheric cyclotron maser in the backward wave oscillator regime, *Radiophys. Quantum Electron.*, *53*(11), 609–622, doi:10.1007/s11141-011-9256-x.
Fu, H. S., J. B. Cao, F. S. Mozer, H. Y. Lu, and B. Yang (2012), Chorus intensification in response to interplanetary shock, *J. Geophys. Res.*, *117*, A01203, doi:10.1029/2011JA016913.
Gao, X., W. Li, R. M. Thorne, J. Bortnik, V. Angelopoulos, Q. Lu, X. Tao, and S. Wang (2014), New evidence for generation mechanisms of discrete and hiss-like whistler mode waves, *Geophys. Res. Lett.*, *41*, 4805–4811, doi:10.1002/2014GL060707.
Horne, R. B., and R. M. Thorne (1998), Potential waves for relativistic electron scattering and stochastic acceleration during magnetic storms, *Geophys. Res. Lett.*, *25*, 3011–3014, doi:10.1029/98GL01002.
Horne, R. B., and R. M. Thorne (2003), Relativistic electron acceleration and precipitation during resonant interactions with whistler-mode chorus, *Geophys. Res. Lett.*, *30*(10), 1527, doi:10.1029/2003GL016973.
Horne, R. B., R. M. Thorne, S. A. Glauert, J. M. Albert, N. P. Meredith, and R. R. Anderson (2005), Timescale for radiation belt electron acceleration by whistler mode chorus waves, *J. Geophys. Res.*, *110*, A03225, doi:10.1029/2004JA010811.
Katoh, Y., and Y. Omura (2007a), Computer simulation of chorus wave generation in the Earth's inner magnetosphere, *Geophys. Res. Lett.*, *34*, L03102, doi:10.1029/2006GL028594.
Katoh, Y., and Y. Omura (2007b), Relativistic particle acceleration in the process of whistler-mode chorus wave generation, *Geophys. Res. Lett.*, *34*, L13102, doi:10.1029/2007GL029758.
Katoh, Y., and Y. Omura (2013), Effect of the background magnetic field inhomogeneity on generation processes of whistler-mode chorus and broadband hiss-like emissions, *J. Geophys. Res. Space Physics*, *118*, 4189–4198, doi:10.1002/jgra.50395.
Keika, K., M. Spasojevic, W. Li, J. Bortnik, Y. Miyoshi, and V. Angelopoulos (2012), PENGUIn/AGO and THEMIS conjugate observations of whistler mode chorus waves in the dayside uniform zone under steady solar wind and quiet geomagnetic conditions, *J. Geophys. Res.*, *117*, A07212, doi:10.1029/2012JA017708.
Kennel, C. F., and H. E. Petschek (1966), Limit on stably trapped particle fluxes, *J. Geophys. Res.*, *71*, 1–28, doi:10.1029/JZ071i001p00001.
Lampe, M., J. Glenn, W. M. Manheimer, and G. Guanuli (2010), Nonlinear whistler instability driven by a beamlike distribution of resonant electrons, *Phys. Plasmas*, *17*, 022902, doi:10.1063/1.3298733.
Le Contel, O., et al. (2008), First results of the THEMIS search coil magnetometers, *Space Sci. Rev.*, *141*(1–4), 509–534, doi:10.1007/s11214-008-9371-y.
Li, W., Y. Y. Shprits, and R. M. Thorne (2007), Dynamic evolution of energetic outer zone electrons due to wave-particle interactions during storms, *J. Geophys. Res.*, *112*, A10220, doi:10.1029/2007JA012368.
Li, W., R. M. Thorne, N. P. Meredith, R. B. Horne, J. Bortnik, Y. Y. Shprits, and B. Ni (2008), Evaluation of whistler mode chorus amplification during an injection event observed on CRRES, *J. Geophys. Res.*, *113*, A09210, doi:10.1029/2008JA013129.
Li, W., R. M. Thorne, V. Angelopoulos, J. W. Bonnell, J. P. McFadden, C. W. Carlson, O. LeContel, A. Roux, K. H. Glassmeier, and H. U. Auster (2009a), Evaluation of whistler-mode chorus intensification on the nightside during an injection event observed on the THEMIS spacecraft, *J. Geophys. Res.*, *114*, A00C14, doi:10.1029/2008JA013554.
Li, W., R. M. Thorne, V. Angelopoulos, J. Bortnik, C. M. Cully, B. Ni, O. LeContel, A. Roux, U. Auster, and W. Magnes (2009b), Global distribution of whistler-mode chorus waves observed on the THEMIS spacecraft, *Geophys. Res. Lett.*, *36*, L09104, doi:10.1029/2009GL037595.
Li, W., et al. (2010a), THEMIS analysis of observed equatorial electron distributions responsible for the chorus excitation, *J. Geophys. Res.*, *115*, A00F11, doi:10.1029/2009JA014845.
Li, W., R. M. Thorne, J. Bortnik, Y. Nishimura, V. Angelopoulos, L. Chen, J. P. McFadden, and J. W. Bonnell (2010b), Global distributions of suprathermal electrons observed on THEMIS and potential mechanisms for access into the plasmasphere, *J. Geophys. Res.*, *115*, A00J10, doi:10.1029/2010JA015687.
Li, W., R. M. Thorne, J. Bortnik, Y. Y. Shprits, Y. Nishimura, V. Angelopoulos, C. C. Chaston, O. LeContel, and J. W. Bonnell (2011), Typical properties of rising and falling tone chorus waves, *Geophys. Res. Lett.*, *38*, L14103, doi:10.1029/2011GL047925.

Li, W., R. Thorne, J. Bortnik, R. McPherron, Y. Nishimura, V. Angelopoulos, and I. G. Richardson (2012), Evolution of chorus waves and their source electrons during storms driven by corotating interaction regions, *J. Geophys. Res.*, *117*, A08209, doi:10.1029/2012JA017797.
Li, W., et al. (2014), Radiation belt electron acceleration by chorus waves during the 17 March 2013 storm, *J. Geophys. Res. Space Physics*, *119*, 4681–4693, doi:10.1002/2014JA019945.
Meredith, N. P., R. B. Horne, and R. R. Anderson (2001), Substorm dependence of chorus amplitudes: Implications for the acceleration of electrons to relativistic energies, *J. Geophys. Res.*, *106*, 13,165–13,178, doi:10.1029/2000JA900156.
Meredith, N. P., R. B. Horne, R. M. Thorne, and R. R. Anderson (2003), Favored regions for chorus-driven electron acceleration to relativistic energies in the Earth's outer radiation belt, *Geophys. Res. Lett.*, *30*(16), 1871, doi:10.1029/2003GL017698.
Meredith, N. P., R. B. Horne, A. Sicard-Piet, D. Boscher, K. H. Yearby, W. Li, and R. M. Thorne (2012), Global model of lower band and upper band chorus from multiple satellite observations, *J. Geophys. Res.*, *117*, A10225, doi:10.1029/2012JA017978.
Meredith, N. P., R. B. Horne, W. Li, R. M. Thorne, and A. Sicard-Piet (2014), Global model of low-frequency chorus (fLHR<f<0.1fce) from multiple satellite observations, *Geophys. Res. Lett.*, *41*, 280–286, doi:10.1002/2013GL059050.
Mourenas, D., A. V. Artemyev, O. V. Agapitov, V. Krasnoselskikh, and F. S. Mozer (2015), Very oblique whistler generation by low-energy electron streams, *J. Geophys. Res. Space Physics*, *120*, 3665–3683, doi:10.1002/2015JA021135.
Ni, B., R. M. Thorne, Y. Y. Shprits, and J. Bortnik (2008), Resonant scattering of plasma sheet electrons by whistler mode chorus: Contribution to diffuse auroral precipitation, *Geophys. Res. Lett.*, *35*, L11106, doi:10.1029/2008GL034032.
Ni, B., R. M. Thorne, Y. Y. Shprits, K. G. Orlova, and N. P. Meredith (2011a), Chorus-driven resonant scattering of diffuse auroral electrons in nondipolar magnetic fields, *J. Geophys. Res.*, *116*, A06225, doi:10.1029/2011JA016453.
Ni, B., R. M. Thorne, N. P. Meredith, R. B. Horne, and Y. Y. Shprits (2011b), Resonant scattering of plasma sheet electrons leading to diffuse auroral precipitation: 2. Evaluation for whistler mode chorus waves, *J. Geophys. Res.*, *116*, A04219, doi:10.1029/2010JA016233.
Ni, B., J. Bortnik, Y. Nishimura, R. M. Thorne, W. Li, V. Angelopoulos, Y. Ebihara, and A. T. Weatherwax (2014), Chorus wave scattering responsible for the Earth's dayside diffuse auroral precipitation: A detailed case study, *J. Geophys. Res. Space Physics*, *119*, 897–908, doi:10.1002/2013JA019507.
Nishimura, Y., et al. (2010), Identifying the driver of pulsating aurora, *Science*, *330*(6000), 81–84, doi:10.1126/science.1193186.
Nishimura, Y., et al. (2013), Structures of dayside whistler mode waves deduced from conjugate diffuse aurora, *J. Geophys. Res. Space Physics*, *118*, 664–673, doi:10.1029/2012JA018242.
Nunn, D., and Y. Omura (2015), A computational and theoretical investigation of nonlinear wave-particle interactions in oblique whistlers, *J. Geophys. Res. Space Physics*, *120*, 2890–2911, doi:10.1002/2014JA020898.
Nunn, D., Y. Omura, H. Matsumoto, I. Nagano, and S. Yagitani (1997), The numerical simulation of VLF chorus and discrete emissions observed on the Geotail satellite using a Vlasov code, *J. Geophys. Res.*, *102*(A12), 27,083–27,097, doi:10.1029/97JA02518.
Omura, Y., and D. Nunn (2011), Triggering process of whistler mode chorus emissions in the magnetosphere, *J. Geophys. Res.*, *116*, A05205, doi:10.1029/2010JA016280.
Omura, Y., Y. Katoh, and D. Summers (2008), Theory and simulation of the generation of whistler-mode chorus, *J. Geophys. Res.*, *113*, A04223, doi:10.1029/2007JA012622.
Omura, Y., M. Hikishima, Y. Katoh, D. Summers, and S. Yagitani (2009), Nonlinear mechanisms of lower-band and upper-band VLF chorus emissions in the magnetosphere, *J. Geophys. Res.*, *114*, A07217, doi:10.1029/2009JA014206.
Parrot, M., and C. A. Gaye (1994), A statistical survey of ELF waves in a geostationary orbit, *Geophys. Res. Lett.*, *21*, 2463–2466, doi:10.1029/94GL01700.
Roux, A., O. LeContel, C. Coillot, A. Bouabdellah, B. de la Porte, D. Alison, S. Ruocco, and M. C. Vassal (2008), The search coil magnetometer for THEMIS, *Space Sci. Rev.*, *141*(1–4), 265–275, doi:10.1007/s11214-008-9455-8.
Santolík, O., D. A. Gurnett, J. S. Pickett, M. Parrot, and N. Cornilleau-Wehrlin (2003), Spatio-temporal structure of storm-time chorus, *J. Geophys. Res.*, *108*(A7), 1278, doi:10.1029/2002JA009791.
Santolík, O., E. Macusova, K. H. Yearby, N. Cornilleau-Wehrlin, and H. S. C. K. Alleyne (2005), Radial variation of whistler-mode chorus: First results from the STAFF/DWP instrument onboard the Double Star TC 1 spacecraft, *Ann. Geophys.*, *23*, 2937–2942.
Santolík, O., D. A. Gurnett, J. S. Pickett, J. Chum, and N. Cornilleau-Wehrlin (2009), Oblique propagation of whistler mode waves in the chorus source region, *J. Geophys. Res.*, *114*, A00F03, doi:10.1029/2009JA014586.
Schriver, D., et al. (2010), Generation of whistler mode emissions in the inner magnetosphere: An event study, *J. Geophys. Res.*, *115*, A00F17, doi:10.1029/2009JA014932.
Shprits, Y. Y., R. M. Thorne, R. B. Horne, S. A. Glauert, M. Cartwright, C. T. Russell, D. N. Baker, and S. G. Kanekal (2006), Acceleration mechanism responsible for the formation of the new radiation belt during the 2003 Halloween solar storm, *Geophys. Res. Lett.*, *33*, L05104, doi:10.1029/2005GL024256.
Shue, J.-H., J. K. Chao, H. C. Fu, C. T. Russell, P. Song, K. K. Khurana, and H. J. Singer (1997), A new functional form to study the solar wind control of the magnetopause size and shape, *J. Geophys. Res.*, *102*, 9497–9511, doi:10.1029/97JA00196.
Shue, J.-H., et al. (1998), Magnetopause location under extreme solar wind conditions, *J. Geophys. Res.*, *103*, 17,691–17,700, doi:10.1029/98JA01103.
Spasojevic, M., and U. S. Inan (2010), Drivers of chorus in the outer dayside magnetosphere, *J. Geophys. Res.*, *115*, A00F09, doi:10.1029/2009JA014452.
Summers, D., R. M. Thorne, and F. Xiao (1998), Relativistic theory of wave-particle resonant diffusion with application to electron acceleration in the magnetosphere, *J. Geophys. Res.*, *103*, 20,487–20,500, doi:10.1029/98JA01740.
Summers, D., C. Ma, N. P. Meredith, R. B. Horne, R. M. Thorne, D. Heynderickx, and R. R. Anderson (2002), Model of the energization of outer-zone electrons by whistler-mode chorus during the October 9, 1990 geomagnetic storm, *Geophys. Res. Lett.*, *29*(24), 2174, doi:10.1029/2002GL016039.
Tao, X. (2014), A numerical study of chorus generation and the related variation of wave intensity using the DAWN code, *J. Geophys. Res. Space Physics*, *119*, 3362–3372, doi:10.1002/2014JA019820.
Tao, X., Q. Lu, S. Wang, and L. Dai (2014), Effects of magnetic field configuration on the day-night asymmetry of chorus occurrence rate: A numerical study, *Geophys. Res. Lett.*, *41*, 6577–6582, doi:10.1002/2014GL061493.
Thorne, R. M. (2010), Radiation belt dynamics: The importance of wave-particle interactions, *Geophys. Res. Lett.*, *37*, L22107, doi:10.1029/2010GL044990.
Thorne, R. M., and C. F. Kennel (1967), Quasi-trapped VLF propagation in the outer magnetosphere, *J. Geophys. Res.*, *72*, 857, doi:10.1029/JZ072i003p00857.
Thorne, R. M., B. Ni, X. Tao, R. B. Horne, and N. P. Meredith (2010), Scattering by chorus waves as the dominant cause of diffuse auroral precipitation, *Nature*, *467*, 943–946, doi:10.1038/nature09467.

Thorne, R. M., et al. (2013), Rapid local acceleration of relativistic radiation-belt electrons by magnetospheric chorus, *Nature*, *504*, 411–414, doi:10.1038/nature12889.

Tsurutani, B. T., and E. J. Smith (1974), Postmidnight chorus: A substorm phenomenon, *J. Geophys. Res.*, *79*, 118–127, doi:10.1029/JA079i001p00118.

Tsurutani, B. T., and E. J. Smith (1977), Two types of magnetospheric ELF chorus and their substorm dependences, *J. Geophys. Res.*, *82*, 5112–5128, doi:10.1029/JA082i032p05112.

Tsurutani, B. T., O. P. Verkhoglyadova, G. S. Lakhina, and S. Yagitani (2009), Properties of dayside outer zone chorus during HILDCAA events: Loss of energetic electrons, *J. Geophys. Res.*, *114*, A03207, doi:10.1029/2008JA013353.

Tsyganenko, N. A., and M. I. Sitnov (2005), Modeling the dynamics of the inner magnetosphere during strong geomagnetic storms, *J. Geophys. Res.*, *110*, A03208, doi:10.1029/2004JA010798.

Tu, W., G. S. Cunningham, Y. Chen, S. K. Morley, G. D. Reeves, J. B. Blake, D. N. Baker, and H. Spence (2014), Event-specific chorus wave and electron seed population models in DREAM3D using the Van Allen Probes, *Geophys. Res. Lett.*, *41*, 1359–1366, doi:10.1002/2013GL058819.

Yue, C., and Q. Zong (2011), Solar wind parameters and geomagnetic indices for four different interplanetary shock/ICME structures, *J. Geophys. Res.*, *116*, A12201, doi:10.1029/2011JA017013.

Yue, C., Q.-G. Zong, and Y. F. Wang (2009), Response of the magnetic field and plasmas at the geosynchronous orbit to interplanetary shock, *Chin. Sci. Bull.*, *54*, 4241–4252, doi:10.1007/s11434-009-0649-6.

Yue, C., Q. G. Zong, H. Zhang, Y. F. Wang, C. J. Yuan, Z. Y. Pu, S. Y. Fu, A. T. Y. Lui, B. Yang, and C. R. Wang (2010), Geomagnetic activity triggered by interplanetary shocks, *J. Geophys. Res.*, *115*, A00I05, doi:10.1029/2010JA015356.

Yue, C., Q. Zong, Y. Wang, I. I. Vogiatzis, Z. Pu, S. Fu, and Q. Shi (2011), Inner magnetosphere plasma characteristics in response to interplanetary shock impacts, *J. Geophys. Res.*, *116*, A11206, doi:10.1029/2011JA016736.

Zong, Q.-G., X.-Z. Zhou, Y. F. Wang, X. Li, P. Song, D. N. Baker, T. A. Fritz, P. W. Daly, M. Dunlop, and A. Pedersen (2009), Energetic electron response to ULF waves induced by interplanetary shocks in the outer radiation belt, *J. Geophys. Res.*, *114*, A10204, doi:10.1029/2009JA014393.